Current Chemistry Letters 10 (2021) 489–502

Contents lists available at GrowingScience

Current Chemistry Letters

homepage: www.GrowingScience.com

The optoelectronic properties of π-conjugated organic molecules based on terphenyl and pyrrole for BHJ solar cells: DFT / TD-DFT theoretical study

M. Raftani[a], T. Abram[a], W. Loued[b], R. Kacimi[a], A. Azaid[a], K. Alimi[b], M. N. Bennani[c] and M. Bouachrine[a,d*]

[a]*Molecular Chemistry and Natural Substances Laboratory, Faculty of Sciences, Moulay Ismail University of Meknes, Morocco*
[b]*Materials Laboratory, Faculty of Science, 5000 Monastir, Tunisia*
[c]*Laboratory of Chemistry and Biology Applied to the Environment, Faculty of Sciences, Moulay Ismail University of Meknes, Morocco*
[d]*EST Khenifra, Sultan Moulay Sliman University, Beni Mellal, Morocco*

C H R O N I C L E

Article history:
Received December 19, 2020
Received in revised form
April 2, 2021
Accepted April 8, 2021
Available online
April 8, 2021

Keywords:
BHJ
Solar cells
Pyrrole
Terphenyl
CAM-B3LYP

A B S T R A C T

In the present paper, four π-conjugated materials, based on terphenyl and pyrrole, with A–D–A structure have been theoretically studied to propose new organic compounds to be used in the organic solar cell field. Moreover, the geometrical and optoelectronic properties of the designed molecules M_1, M_2, M_3 and M_4 have been computed after optimization in their fundamental states, using the quantum chemical method DFT / B3LYP/ 6−311G (d, p). Different parameters including HOMO and LUMO energy levels, bandgap energy, frontier molecular orbital (FMO), chemical reactivity indices, the density of states (DOS), V_{oc}, electrostatic potential (ESP), and thermodynamic parameters at several temperatures in the range of 0-500 K have been determined. The absorption properties including the transition energy, the wavelengths (λ_{max}), the excitation vertical energy, and the corresponding oscillator strengths of these molecules have been studied using the quantum chemical method TD−DFT / CAM–B3LYP / 6–311G (d, p). The obtained results of our studied compounds show that M_3 (with *2H,* 2'H-1, 1'-biisoindole moiety) as a donor group has special optoelectronic, absorption, and good photovoltaic characteristics. Thus, they can be utilized as an electron-donating in organic solar cells BHJ type.

1. Introduction

In the last few years, organic solar cells have supplied remarkable importance to researchers because they present special characteristics including lightweight, fabrication possibility on flexible substrates, and high throughput.[1] Various researchers are condensing their efforts into synthesizing molecules with small chains based on π-conjugated compounds since the structure of these compounds is not amorphous and can be manufactured with determined structures.[2] These materials operate as fitting candidates for studying low-cost organic photovoltaic apparatus,[3] due to their special characteristics; taking as examples photochemical, thermal stability, charge mobility.[4] Let's recall that the π-conjugated compounds are broadly used in different applications[5] such as OFET,[6] OLEDs[7] and organic

* Corresponding author.
E-mail address: m.bouachrine@est-umi.ac.ma (M. Bouachrine)

doi: 10.5267/j.ccl.2021.4.002

solar cell.[8] A conjugated material contains an alternation of single and dual bonds, this leads to the delocalization of π electrons on the monomer units.[9] The presence of π electrons makes these molecules electron donors. By absorbing emitted photons, these electrons can be excited from the HOMO level to the LUMO.[4] Because of their important particular characteristics,[10] our molecules have become favorable materials for polymer solar cells (PSC).[11]

PSCs lean on the concept of bulk heterojunction (BHJ) because of their ease of manufacture, the low cost of fabrication, the lightweight, and attractive flexibility.[12, 13] The architecture of a BHJ organic solar cell consists mainly of a π-conjugated material as a donor and a fullerene derivative ([6, 6]-phenyl-C_{61}-butyric acid methyl ester) PCBM-C_{60})[14] as an acceptor.[15] A more efficient generation of charge carriers is the function of such organic solar cell BHJ type.[3]

Among the various materials designed for BHJ solar cell devices, π-conjugated polymers are based on polyaniline, polythiophene, polyphenyl, and polypyrrole.[16-18] Several studies are interested in polypyrrole because it owns interesting properties like stability, excellent conductivity, and facility of manufacture by chemical or electrochemical polymerizations.[19]

In this, we have implemented a theoretical investigation of the geometric and optoelectronic parameters of π-conjugated materials based on terphenyl and pyrrole with the structure A–D–A. In fact, four molecules named M_1, M_2, M_3, and M_4 have been studied. The structure of these four compounds is shown in **Fig. 1**. The fundamental state and geometry of these compounds are optimized by the quantum method DFT at B3LYP/6-311G (d, p) basis set.[20, 21] The two methods DFT and TD-DFT were used aiming to study their electronic and absorption properties. Finally, the thermodynamic parameters of the optimized structures have been theoretically computed based on the vibration's analysis.

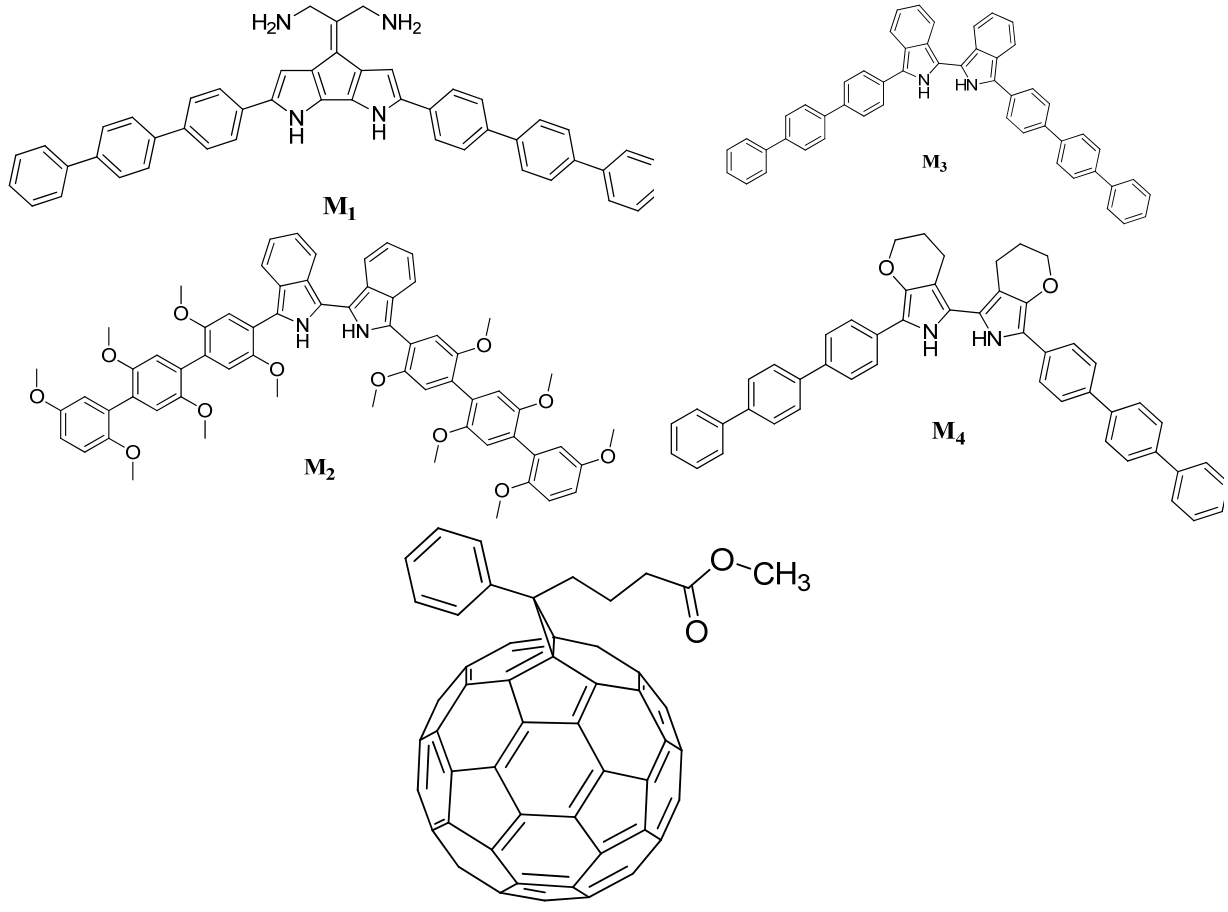

Fig. 1. Structures of the M_i compounds and fullerene derivative (PCBM).

2. Computational methods

The quantum chemical method DFT at B3LYP,[22-24] with the 6–311G (d, p) basis set,[25-27] has been employed for all calculations. All of these calculations are done via the Gaussian 09 software.[28] The optimization of the geometric structure for our compounds in the fundamental state is realized. From the stable structure of the fundamental state, the HOMO and LUMO energy levels, and bandgap energy[29] have been determined. The density of states (DOS) distribution has been visualized using the GaussSum software.[30] The thermodynamic parameters such as entropy (S), internal energy (U), enthalpy (H), and free energy (G) have been investigated at the various temperatures in the range of 0-500 K, based on vibrational frequency computations by DFT/B3LYP/6311g (d, p) method. Here, different parameters such as the wavelengths (λ_{max}), the corresponding oscillator strengths, and the excitation energy of our studied compounds have been realized in their fundamental state geometries by the TD−DFT/CAM–B3LYP/6–311 G (d, p).[31]

3. Results and discussion

3.1. Geometrical properties

To define the geometrical properties as the bond lengths (Å) and dihedral angles (θº), quantum chemical method DFT/B3LYP/6−311G (d, p) is applied to optimize our investigated compounds M_i (i=1-4) in their fundamental state. **Fig.** 2 displays optimized geometries of our investigated molecules and **Table** 1 exhibits their parameters (d_i and θ_i).

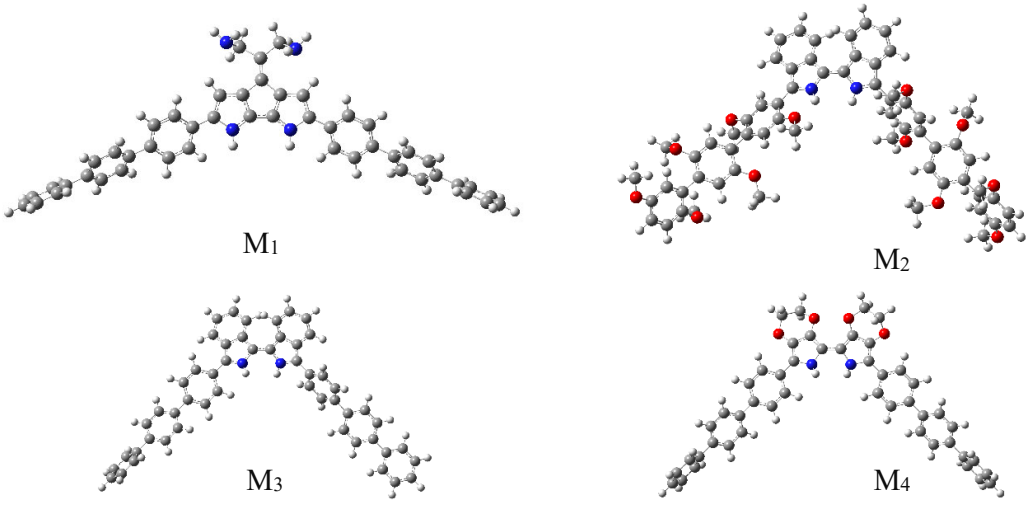

Fig. 2: The optimized structure of the molecules M_i

Table 1. The selected parameters d_i (Å) and θ_i (º) for M_i molecules at DFT/B3LYP/6−311G (d, p)

Compound	d_1	d_2	d_3	d_4	d_5	d_6	θ_1	θ_2	θ_3	θ_4	θ_5	θ_6
M_1	1.48	1.48	1.45	1.45	1.48	1.48	140.74	142.96	160.63	159.04	142.79	140.69
M_2	1.49	1.49	1.46	1.46	1.49	1.49	132.68	130.22	156.88	145.34	130.89	128.70
M_3	1.48	1.48	1.45	1.45	1.48	1.48	140.60	142.63	151.28	150.36	142.64	141.21
M_4	1.48	1.48	1.45	1.45	1.48	1.48	140.74	143.42	167.75	166.20	143.66	140.96

In this context, the bond length values (d_i) for the four compounds vary from 1.45 Å to 1.48 Å. It is noticed that the bond lengths (d_i) decrease when they approach the pyrrole unit in all molecules and do not know a significant variation.[4] According to these results, it is indicated that these bonds tend towards single ones and have a C–C character (~1.5Å).[32] This makes intramolecular charge transfer (ICT) easily betwixt the units forming each molecule. The optimized structure for all molecules reveals that the dihedral angles have values between 140° and 167 ° from the findings mentioned in **Table 1**, suggesting that these compounds have twisted configurations.[5]

3.2. Optoelectronic properties

To study such an organic solar cell, it is necessary to know the energy levels of HOMO and LUMO.[33] Therefore, the energy levels of HOMO and LUMO represent a major role in deciding if a successful charge transfer can occur betwixt the donor and the acceptor.[34] Electronic parameters such as E_{LUMO}, E_{HOMO}, and E_{gap} ($E_{gap} = E_{LUMO} - E_{HOMO}$) for the studied compounds have been theoretically determined based on the DFT/B3LYP/6−311G (d, p) method. To transfer electrons easily betwixt the levels of HOMO and LUMO when the material absorbs light, it is necessary to have a small bandgap value.[4] **Table** 2 exhibits the computed energies of the studied compounds M_i: E_{gap}, E_{LUMO}, and E_{HOMO}.

Table. 2. the computed energies of electronic parameters obtained by DFT/ B3LYP/6−311G (d, p)

Compounds	$-E_{HOMO}$ (eV)	$-E_{LUMO}$ (eV)	E_{gap} (eV)
M_1	4.39	1.53	2.86
M_2	4.39	1.64	2.76
M_3	4.56	1.84	2.73
M_4	4.50	1.55	2.95

It has been shown by several researchers that the energy levels of HOMO, LUMO, and the bandgap of a π-conjugated molecule are characteristically dependent on the length of the chain.[35] It is noted that in π-conjugated compounds, the increase in the length of the conjugation leads to destabilizing HOMO energy and to stabilizing LUMO energy.[36] As mentioned in **Table** 2 above, the E_{HOMO} / E_{LUMO} energies values are -4.392 eV/-1.53 eV for M_1, -4.39 eV/-1.64 eV for M_2, -4.56 eV/-1.84 eV for M_3 and -4.50 eV/-1.55 eV for M_4. The corresponding band gap values (E_{gap}) range between 2.73 eV and 2.95 eV and are decreased as follows: M_4 (2.95 eV) > M_1 (2.86 eV) > M_2 (2.76 eV) > M_3 (2.73 eV). On the other hand, this decrease is attached to the presence of the biisoindole group, which conducts to decreasing the E_{HOMO} and increasing the E_{LUMO}; this leads to decreasing E_{gap}.[37]

To clearly inform on the excitation properties and the ICT for the π-conjugated systems, a study of HOMO and LUMO of our oligomers is important.[38] Therefore, based on the method DFT/B3LYP/6−311G (d, p), the HOMO and LUMO orbitals of these compounds have been carried out from the optimized structure.[5] The frontier molecular orbitals (FMO) for these compounds are displayed in **Fig. 3**. It is remarked from **Fig. 3** that the electron density of all orbitals HOMO has relatively an analogous character and is localized on the donor moieties; whereas, the electron density of all orbitals LUMO is distributed on the terphenyl moieties (acceptor group). The LUMO's density is distributed over all the π-conjugated molecules. Generally, the FMO of all compounds has similar distribution characteristics; for example, the HOMO's have a π-bonding character in the subunits and a π-antibonding character betwixt the consecutive subunits,[39] while the LUMO's usually own a π-antibonding character inside the subunit and a π-bonding character between the subunits.[40]

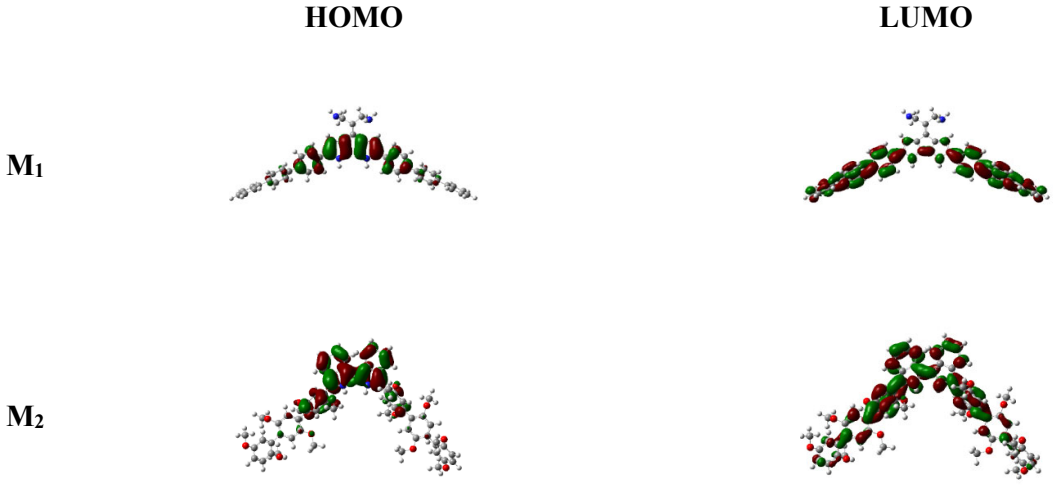

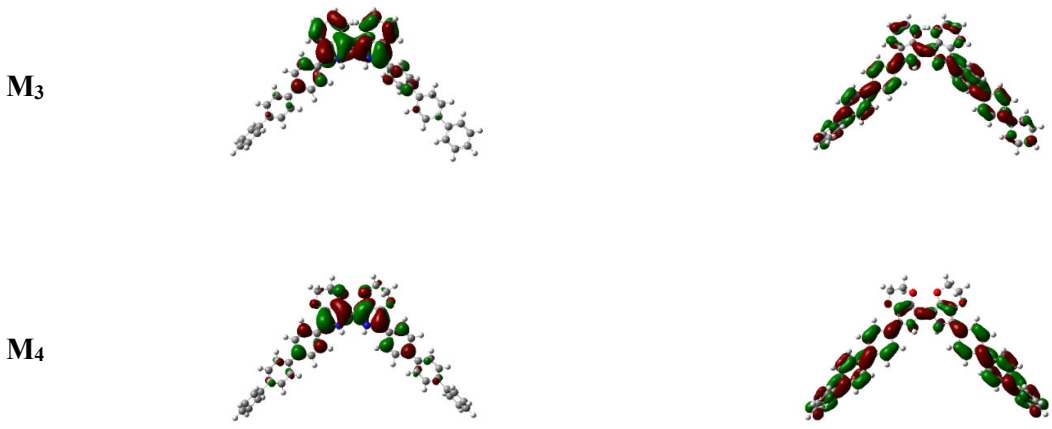

Fig. 3: The contour plots of HOMO and LUMO orbitals for the studied compounds

3.3. Chemical reactivity indices

Several global reactivity parameters have been introduced in the chemical literature[41] such as electronegativity (**χ),**[42] hardness (η),[43, 44] electrophilicity index (ω),[45] and the chemical potential (μ). On the base of the energy values of HOMO and LUMO orbitals for such compound, chemical reactivity indices parameters can be calculated via the following formulas: [46, 47]

- Chemical potential : $\mu = (E_{HOMO} + E_{LUMO})/2$;
- Hardness : $\eta = (E_{LUMO} - E_{HOMO})/2$;
- Electronegativity : $\chi = -(E_{HOMO} + E_{LUMO})/2$;
- Electrophilicity index: $\omega = \mu^2/2\eta$

Table. 3. The calculated chemical reactivity indices (all in eV) for the M_i molecules and PCBM.

Compounds	η	μ	χ	ω
M_1	1.43	-2.96	2.96	6.27
M_2	1.38	-3.01	3.01	6.26
M_3	1.36	-3.20	3.20	6.98
M_4	1.48	-3.02	3.02	6.74
PCBM	1.20	-4.90	4.90	14.41

The results referred in **Table** 3 exhibit that the PCBM has the tiniest chemical potential value (μ = -4.90) relative to the other compounds examined, suggesting that the electrons can readily rap out from the donor compounds of the BHJ solar cell to the PCBM, which is a strong acceptor. As regards electronegativity (χ), it can be observed that the PCBM possesses a high value compared to other compounds. This implies that the latter has the potential to draw the electrons of other substances towards it. On the other hand, the PCBM has the lowest chemical hardness value (almost). This indicates that it is very difficult for the PCBM to release electrons. However, these molecules are better for easily releasing electrons. The findings then exhibit that electrophilicity values are lower relative to PCBM in the investigated molecules. This indicates that these molecules are good electron donors. Finally, in the BHJ type solar cells, we infer that these molecules can act as better electron donors, whereas the PCBM is a good electron acceptor.

3.4. The density of states (DOS)

A BHJ solar cell consists of disordered semiconductors and materials with localized band tail states.[48] In BHJ, carriers have dispersive mobility, while electron transport is controlled by the acceptor, and the holes are carried by the donor,[48] although both carriers can move easily between the two

materials. The density of states (DOS) study is therefore important because this parameter is the connection betwixt the structure of the BHJ solar cell and its electronic characteristics.[48] Recent work has shown that the density of states (DOS) can explain charge transport properties in semiconductor materials. The DOS is indispensable for the study of electrons at the valence and conduction bands (α and β electrons), whereas this parameter is valid just for the free electrons. The DOS distribution is determined with the GaussSum application and is displayed in **Fig. 4**. The lines at the end of the x-axis with energy between -20 eV and -2 eV are filled orbitals, whereas those between -2 eV and 0 eV are considered empty orbitals. An empty orbital is called an acceptor one, while the donor orbital is the occupied one. At specific energy levels, a high-intensity density of states (DOS) signifies that several states are available to be occupied, whereas a zero-intensity DOS implies that the system cannot occupy any state.[49]

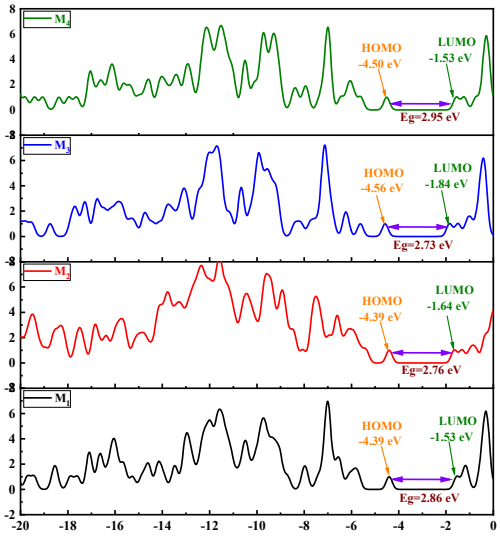

Fig. 4. DOS of the M_1 M_2, M_3, and M_4, compounds

3.5. Molecular electrostatic potential (MEP) analysis

The electrostatic molecular potential (MEP) is a three-dimensional graphical representation on a surface with constant electrical density.[50] MEP maps illustrate the distribution of the nuclear and electronic charges of molecules.[51] They are used for chemical reactivity prediction (electrophilic attacks and nucleophilic ones) and hydrogen bond interplay.[52] The molecular electrostatic potential is determined via the quantum chemical method DFT-B3LYP/6−311G (d, p). **Fig. 5** displays MEP surfaces. Also, the electrostatic potential values in the MEP maps are shown in three colors: blue, red, and green.[51] The color code of the map is between - 0.149 e^0 and 0.149 e^0, - 0.167 e^{-0} and 0.167 e^{-0}, - 0.151 e^{-0} and 0.151 e^{-0} and - 0.112 e^{-0} and 0.112 e^{-0} for the molecules M_1, M_2, M_3 and M_4 respectively.[38]

It is remarked that the electrostatic potential values as mentioned above, seem with several colors, where the red color in a map corresponds to a region rich in electrons (negative), the electron-deficient zone (positive) is colored in blue, while the region with zero potential is in green.[53] It is observed from **Fig.** 5 that the blue-colored region (electron-deficient area) is localized on the pyrrole ring. Therefore, the terphenyl group is electropositive. This indicates that this group can be deemed as a suitable donor. Furthermore, it is noticed that the rest of the units are surrounded by a null potential.[4]

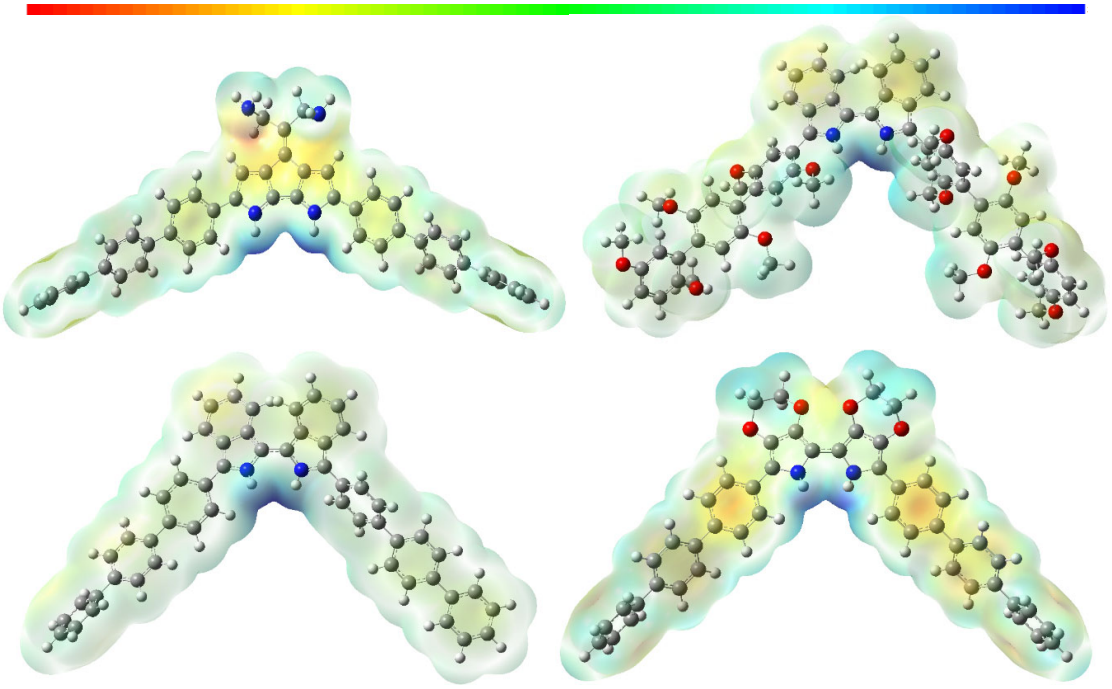

Fig. ۵. MEP surfaces of the four M_i compounds

3.6. Photovoltaic properties

Commonly, the parameter widely used to analyze the performances of such an organic solar cell is the power conversion efficiency (PCE).[33] Consequently, in the study of their photovoltaic characteristics, the energy levels of both orbitals HOMO and LUMO of the acceptor and donor compounds are considered as essential factors. In this work, a photovoltaic study of the studied compounds is performed. Calculations of the electronic parameters (LUMO and HOMO) for the M_i molecules are performed via the DFT method with B3LYP / 6–311G (d, p) from their optimized structures. These two parameters (HOMO and LUMO) help to define the photovoltaic properties of the studied compounds, such as energy corresponding to the open-circuit voltage (V_{oc}), short circuit current, and fill factor.

The energy corresponding to the open-circuit voltage (V_{oc}) of the bulk heterojunction (BHJ) Solar cell may be theoretically calculated as the difference between the donor's HOMO energy level (M_i) and the acceptor's LUMO ones (PCBM),[54] taking into account the energy lost during the photo-charge generation.[55] The latter parameter can be expressed as follows (Eq. (1)):[56]

$$V_{oc} = \frac{1}{e}\left(\left| E_{HOMO}^{Donor} \right| - \left| E_{LUMO}^{Acceptor} \right| - 0.3 \right), \quad (1)$$

where E_{HOMO}^{Donor} is the energy level of the donor M_i, $E_{LUMO}^{Acceptor}$ is the energy level of the acceptor and 0.3 V presents the empirical value for V_{OC} losses[57] proposed by Scharber and his collaborators who proposed equations (1) and (2). Different studies suggested that the physical reasons for this 0.3 V loss factor emphasize the impact of the disorder on the maximum achievable V_{OC} in organic solar cells.[58, 59] Durrant and his collaborators[60, 61] identify the effect of charge carrier recombination and the structure of the donor-acceptor blend on the V_{OC} in bulk heterojunction solar cells. Based on an analysis of transient optoelectronic studies, a model has been developed to predict the open-circuit voltage of BHJ devices. They found for different polymer fullerene solar cells open circuit voltage losses in the range of 0.225–0.435 V.[62]

For each couple (Donor/acceptor), we have determined the value of the parameter ΔE_{LUMO} using the following expression:

$$\Delta E_{LUMO} = |E_{LUMO}^{Donor}| - |E_{LUMO}^{Acceptor}|, \quad (2)$$

where E_{LUMO}^{Donor} is the energy level of the donor M_i and $E_{LUMO}^{Acceptor}$ is the energy level of the derivative fullerene acceptor. In order to own high solar cell efficiency, a high V_{oc} value is needed. For this, the π-conjugated compounds must have a low LUMO energy, and the electron acceptor (PCBM) must have a high LUMO one.[51] The obtained results of the two parameters cited in equations (2) and (3) are shown in **Table 4**.

Table. 4: Energy values obtained with B3LYP / 6−311G (d, p) of E_{gap}, V_{oc} and ΔE_{LUMO}

Compounds	E_{HOMO} (eV)	E_{LUMO} (eV)	E_{gap} (eV)	V_{oc} (V)	ΔE_{LUMO} (eV)
M_1	-4.39	-1.53	2.86	0.39	2.17
M_2	-4.39	-1.64	2.76	0.39	2.06
M_3	-4.56	-1.84	2.73	0.56	1.86
M_4	-4.50	-1.55	2.95	0.50	2.15

It is noted from the results in **Table 4** that the V_{oc} values for our molecules M_1, M_2, M_3, and M_4 are 0.39 V, 0.39 V, 0.56 V, and 0.50 V respectively. This indicates that these values are sufficient for the electrons to be injected into the unoccupied orbital of the acceptor. Besides, the LUMO energy differences (ΔE_{LUMO}) values betwixt the occupied orbitals and the unoccupied ones vary from 1.86 to 2.17 eV. This assures an electron transfer between the donors and the acceptor. As a result, these compounds may be used as a BHJ solar cell because of their ability to inject the valence band electrons (excited molecules) into the conduction band (PCBM).[63]

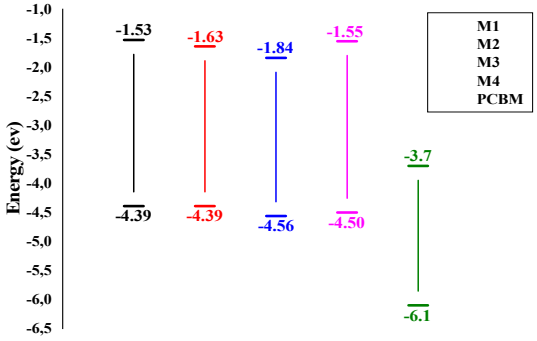

Fig. 6. Diagram of HOMO and LOMO energy of studied molecules and acceptor PCBM

3.7. Absorption properties

To study the excited states absorption spectra,[64] TD−DFT computations at CAM−B3LYP/6−311G (d, p) have been performed. This functional (CAM−B3LYP) is considered the best instrument to prophesy the optical properties of conjugated organic materials[65] because it presents a good agreement between the UV-vis spectra predicted by this functional and those measured experimentally.[66] Therefore, the absorption properties such as electronic vertical transition energy, oscillator strengths, maximum absorption wavelength, and nature of the transitions have been computed with CAM−B3LYP/6−311G (d, p). The obtained data of absorption have been collected in **Table 5** and the corresponding spectra are displayed in **Fig. 7**.

Table. 5. Absorption spectral data of M_i molecules obtained by CAM−B3LYP/6−311G (d, p)

compounds	λ_{abs} (nm)	E_{tr} (eV)	f	Assignment
M_1	506.99	2.45	0.90	H → L (73%)
M_2	513.90	2.41	1.00	H → L (99%)
M_3	514.43	2.41	1.11	H → L (99%)
M_4	472.41	2.62	1.44	H → L (99%)

The obtained results in **Table 5** show that the strongest absorption in UV-visible (λ_{max}>400 nm) for these compounds generally corresponds to the electronic transition HOMO → LUMO.[55] It is noted that this absorption consists of the transition of the π bonding to the π^* anti-bonding (π-π^* transition).[67] As displayed in **Fig. 6**, every compound exhibits a single band. The great intensive band is situated in region 340 – 730 nm, which consists of π-π^* transition in aromatic groups of the complete molecule. Moreover, it is remarked that for all compounds, the absorption area varies from 472 nm to 514 nm. Thus, the maximum absorption wavelength has been observed in compound M_3; whereas, through **Table 5**, it is observed that the calculated wavelength of the studied compounds decreases as follows: M_3 (514 nm) > M_2 (513 nm) > M_1 (506 nm) > M_4 (472 nm). This bathochromic effect shift of the four compounds can be explained by better delocalization of electrons permitted by the atoms oxygen and nitrogen toward relation to the carbon ones.[55]

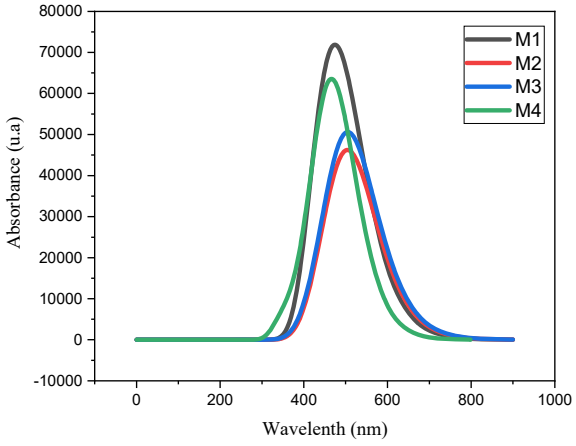

Fig. 7: Absorption spectra for the M_i molecules obtained by CAM-B3LYP/6-311G (d, p)

3.8. Thermodynamic properties

On the base of vibrational analysis at DFT/B3LYP/6-311G (d, p) level, the standard statistical thermodynamic functions: entropy (S), internal energy (U), enthalpy (H), and free energy (G) for the title polymers were obtained from the theoretical harmonic functions and all thermodynamic calculations were done in the gas phase. **Fig. 8** depicts the correlation of S, U, H, and G with temperature. It could be seen that these thermodynamic functions (S, U, and H), except the free energy (G), are increasing with temperature varying from 100 to 500 K. This is explained by the fact that the vibrational intensities rise with temperature.[68] However, it is noted that the chain length does not affect the calculated results. However, the calculated entropy, internal energy, and enthalpy increase with the increase of chain length. The negative value of free energy means that the reaction is thermodynamically favorable and spontaneous.

The correlation equations between entropy, internal energy, enthalpy, free energy changes, and temperatures have been fitted by quadratic formulas as follows:

$S = 279.06459 + 0.46508\ T - 5.50423\times10^{-4}\ T^2$ (R= 0.9485, SD = 6.85246)

$U = -5.88776\times10^{-5} + 0.02494\ T - 7.04128\times\ 10^{-10}\ T^2$ (R= 1, SD = 2.98627×10^{-4})

$H = 1.78571\times10^{-5} + 0.03326\ T - 1.5006 \times 10^{-10}\ T^2$ (R= 1, SD = 2.95968×10^{-4})

$G = 2.2747 - 0.31417\ T - 8.00565\times10^{-5}\ T^2$ (R= 0.99995, SD = 0.36922)

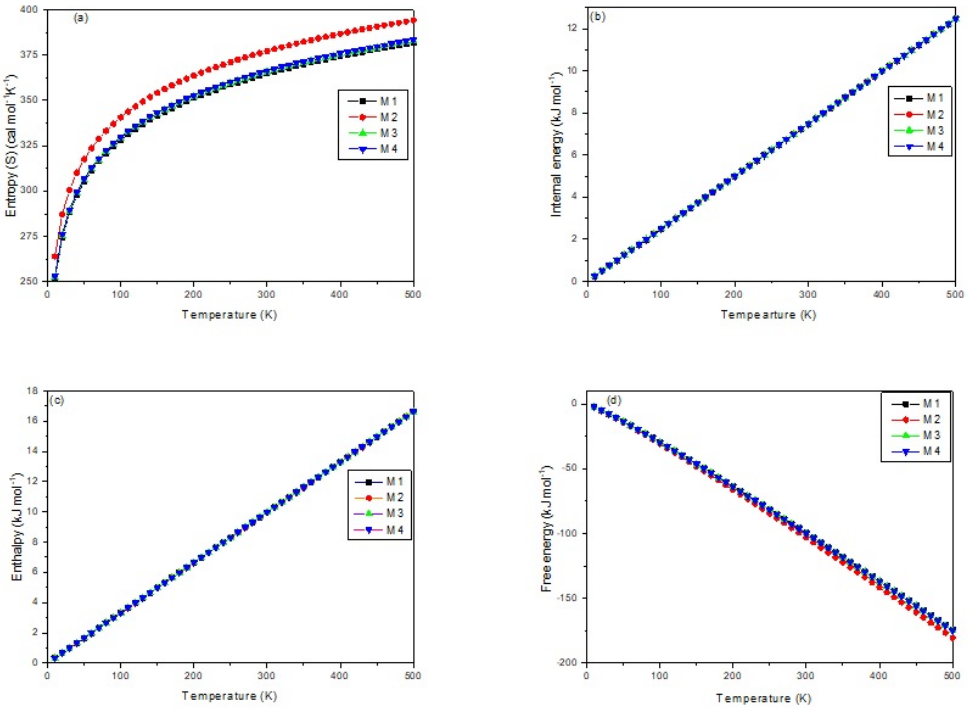

Fig. 8. Correlations graphic (a) between entropy and temperature, (b) between internal energy and temperature, (c) between enthalpy and temperature, and (d) between free energy and temperature

The corresponding fitting equations with fitting factors (R^2) for these thermodynamic properties (S, U, H, and G) are 0.9485, 1, 1, and 0.99995, respectively. Standard deviation (SD) values for these thermodynamic properties are 6.85246, 2.98627×10^{-4}, $2.95968\times10^{-4,}$ and 0.36922, respectively. All the thermodynamic data supply helpful information for the further study of these compounds and estimate the direction of chemical reactions according to the second law of thermodynamics.[69]

4. Conclusion

In conclusion, the quantum method DFT and its TD-DFT approaches are used to optimize the geometrical structure of new conjugated molecules based on terphenyl and pyrrole with an A-D-A structure for application in BHJ solar cells. Also, this quantum method is relied on to theoretically calculate their electronic, photovoltaic, and optical properties. Besides, the aim is to see the donor effects on the parameters d_i, θ_i, E_{HOMO}, E_{LUMO}, E_{gap}, V_{oc}, λ_{max}, and chemical reactivity indices of the cell. The obtained results show that the band gaps of our studied compounds range between 2.73 eV and 2.95 eV. This indicates that these molecules possess a high order of conjugation. On the other hand, it is observed that the better V_{oc} values designated for the M_i molecules blend with the acceptor PCBM. For our studied compounds, the computed V_{oc} values are between 0.39 V and 0.56 V, suggesting that these values are enough for possible effective electron injection. The computed absorption spectra of these four compounds exhibit an electronic transition HOMO → LUMO (π–π* type). It is observed that the absorption peaks for our studied compounds vary from 472 nm to 514 nm. Furthermore, the thermodynamic parameters (entropy, internal energy, enthalpy, and free energy) rise with the increase of the temperature which varies from 100 to 500 K by dint of the fact that the vibrational intensities rise with temperature. This can make them suitable to harvest light effectively.

References

1 Rafique S., Abdullah S. M., Sulaiman K., and Iwamoto M. (**2018**) Fundamentals of bulk heterojunction organic solar cells: An overview of stability/degradation issues and strategies for improvement. *Renewable and Sustainable Energy Reviews,* 84 (December 2017), 43-53.

2 Wu W., Liu Y., and Zhu D. (**2010**) Π-conjugated molecules with fused rings for organic field-effect transistors: Design, synthesis and applications. *Chemical Society Reviews,* 39 (5), 1489-1502.

3 Derouiche H., and Djara V. (**2007**) Impact of the energy difference in lumo and homo of the bulk heterojunctions components on the efficiency of organic solar cells. *Solar Energy Materials and Solar Cells,* 91 (13), 1163-1167.

4 Bourass M., Touimi Benjelloun A., Benzakour M., Mcharfi M., Jhilal F., Serein-Spirau F., Marc Sotiropoulos J., and Bouachrine M. (**2017**) Dft/td-dft characterization of conjugational electronic structures and spectral properties of materials based on thieno[3,2-b][1]benzothiophene for organic photovoltaic and solar cell applications. *Journal of Saudi Chemical Society,* 21 (5), 563-574.

5 Raftani M., Abram T., Kacimi R., Bennani M. N., and Bouachrine M. (**2020**) Organic compounds based on pyrrole and terphenyl for organic light-emitting diodes (oled) applications : Design and electro-optical properties. *Journal of Materials and Environmental Sciences,* 11 (4), 933-946.

6 Chen H., Cui Q., Yu G., Guo Y., Huang J., Zhu M., Guo X., and Liu Y. (**2011**) Synthesis and characterization of novel semiconductors based on thieno[3,2- b][1]benzothiophene cores and their applications in the organic thin-film transistors. *Journal of Physical Chemistry C,* 115 (48), 23984-23991.

7 Azrain M. R., Mansor M. R., Omar G., Fadzullah S. H. S. M., Esa S. R., Lim L. M., Sivakumar D., and Nordin M. N. A. (**2019**) Effect of high thermal stress on the organic light emitting diodes (oleds) performances. *Synthetic Metals,* 247, 191-201.

8 Ebata H., Miyazaki E., Yamamoto T., and Takimiya K. (**2007**) Synthesis, properties, and structures of benzo[1,2-b:4,5-b′]bis[b] benzothiophene and benzo[1,2-b:4,5-b′]bis[b]benzoselenophene. *Organic Letters,* 9 (22), 4499-4502.

9 Grozema F. C., Candeias L. P., Swart M., Van Duijnen P. T., Wildeman J., Hadziioanou G., Siebbeles L. D. A., and Warman J. M. (**2002**) Theoretical and experimental studies of the opto-electronic properties of positively charged oligo(phenylene vinylene)s: Effects of chain length and alkoxy substitution. *Journal of Chemical Physics,* 117 (24), 11366-11378.

10 Hasnaoui K., Zgou H., Hamidi M., and Bouachrine M. (**2008**) New materials based on carbazole for optoelectronic device applications: Theoretical investigation. *Chinese Chemical Letters,* 19 (4), 488-492.

11 Krebs F. C., Jørgensen M., Norrman K., Hagemann O., Alstrup J., Nielsen T. D., Fyenbo J., Larsen K., and Kristensen J. (**2009**) A complete process for production of flexible large area polymer solar cells entirely using screen printing-first public demonstration. *Solar Energy Materials and Solar Cells,* 93 (4), 422-441.

12 Tanguy L., Malhotra P., Singh S. P., Brisard G., Sharma G. D., and Harvey P. D. (**2019**) A 9.16% power conversion efficiency organic solar cell with a porphyrin conjugated polymer using a nonfullerene acceptor. *ACS Applied Materials and Interfaces,* 11 (31), 28078-28087.

13 Huang X., Hu M., Zhao X., Li C., Yuan Z., Liu X., Cai C., Zhang Y., Hu Y., and Chen Y. (**2019**) Subphthalocyanine triimides: Solution processable bowl-shaped acceptors for bulk heterojunction solar cells. *Organic Letters,* 21 (9), 3382-3386.

14 Wang H., He Y., Li Y., and Su H. (**2012**) Photophysical and electronic properties of five pcbm-like c 60 derivatives: Spectral and quantum chemical view. *Journal of Physical Chemistry A,* 116 (1), 255-262.

15 Morvillo P. (**2009**) Higher fullerenes as electron acceptors for polymer solar cells: A quantum chemical study. *Solar Energy Materials and Solar Cells,* 93 (10), 1827-1832.

16 Lee K., Cho S., Sung H. P., Heeger A. J., Lee C. W., and Lee S. H. (**2006**) Metallic transport in polyaniline. *Nature,* 441 (1), 65-68.

17 Zhang F., Halverson P. A., Lunt B., and Linford M. R. (**2006**) Wet spinning of pre-doped polyaniline into an aqueous solution of a polyelectrolyte. *Synthetic Metals,* 156 (14-15), 932-937.

18 Song H. K., and Palmore G. T. R. (**2006**) Redox-active polypyrrole: Toward polymer-based batteries. *Advanced Materials,* 18 (13), 1764-1768.

19 Nguyen V. C., and Potje-Kamloth K. (**1999**) Electrical and chemical sensing properties of doped polypyrrole/gold schottky barrier diodes. *Thin Solid Films,* 338 (1-2), 142-148.

20 Witwicki M., and Jezierska J. (**2010**) Protic and aprotic solvent effect on molecular properties and g-tensors of o-semiquinones with various aromacity and heteroatoms: A dft study. *Chemical Physics Letters,* 493 (4-6), 364-370.

21 Raftani M., Abram T., Azaid A., Kacimi R., Bennani M. N., and Bouachrine M. (**2021**) Theoretical design of new organic compounds based on diketopyrrolopyrrole and phenyl for organic bulk heterojunction solar cell applications: Dft and td-dft study. *Materials Today: Proceedings*.

22 Becke A. D. (**1993**) A new mixing of hartree-fock and local density-functional theories. *The Journal of Chemical Physics,* 98 (2), 1372-1377.

23 Vessally E., Siadati S. A., Hosseinian A., and Edjlali L. (**2017**) Selective sensing of ozone and the chemically active gaseous species of the troposphere by using the c20 fullerene and graphene segment. *Talanta,* 162 (October 2016), 505-510.

24 Siadati S. A., Amini-Fazl M. S., and Babanezhad E. (**2016**) The possibility of sensing and inactivating the hazardous air pollutant species via adsorption and their [2 + 3] cycloaddition reactions with c20 fullerene. *Sensors and Actuators, B: Chemical,* 237, 591-596.

25 Wong M. W., Gill P. M. W., Nobes R. H., and Radom L. (**1988**) 6-311g(mc)(d,p): A second-row analogue of the 6-311g(d,p) basis set. Calculated heats of formation for second-row hydrides. *Journal of Physical Chemistry,* 92 (17), 4875-4880.

26 Siadati S. A., Vessally E., Hosseinian A., and Edjlali L. (**2016**) Possibility of sensing, adsorbing, and destructing the tabun-2d-skeletal (tabun nerve agent) by c20 fullerene and its boron and nitrogen doped derivatives. *Synthetic Metals,* 220, 606-611.

27 S.A. Siadati S. R. (**2018**) Switching behavior of an actuator containing germanium, silicon-decorated and normal c20 fullerene. *Chemical Review and Letters,* 1, 77-81.

28 Frisch M. J., Trucks G. W., Schlegel H. B., Scuseria G. E., Robb M. A., Cheeseman J. R., Scalmani G., Barone V., Mennucci B., Petersson G. A., Nakatsuji H., Caricato M., Li X., Hratchian H. P., Izmaylov A. F., Bloino J., Zheng G., Sonnenberg J. L., Hada M., Ehara M., Toyota K., Fukuda R., Hasegawa J., Ishida M., Nakajima T., Honda Y., Kitao O., Nakai H., Vreven T., Montgomery Jr J. A., Peralta J. E., Ogliaro F., Bearpark M., Heyd J. J., Brothers E., Kudin K. N., Staroverov V. N., Kobayashi R., Normand J., Raghavachari K., Rendell A., Burant J. C., Iyengar S. S., Tomasi J., Cossi M., Rega N., Millam J. M., Klene M., Knox J. E., Cross J. B., Bakken V., Adamo C., Jaramillo J., Gomperts R., Stratmann R. E., Yazyev O., Austin A. J., Cammi R., Pomelli C., Ochterski J. W., Martin R. L., Morokuma K., Zakrzewski V. G., Voth G. A., Salvador P., Dannenberg J. J., Dapprich S., Daniels A. D., Farkas Ö., Foresman J. B., Ortiz J. V., Cioslowski J., and Fox D. J. (**2009**) Gaussian 09, rev. A.02.

29 Pakravan P., and Siadati S. A. (**2017**) The possibility of using c20 fullerene and graphene as semiconductor segments for detection, and destruction of cyanogen-chloride chemical agent. *Journal of Molecular Graphics and Modelling,* 75 (2017), 80-84.

30 Noel M. O'boyle A. L. T., and Karol M L. (**2012**) Software news and updates gabedit — a graphical user interface for computational chemistry softwares. *Journal of computational chemistry,* 32, 174-182.

31 L.Yan, Y.Lu, and X.Li (**2016**) A density functional theory protocol for the calculation of redox potentials of copper complexes complexes. *Electronic Supplementary Material,* 18, 5529-5536.

32 De Athayde-Filho P. F., Miller J., Simas A. M., Lira B. F, De Souza Luis J. A., and Zuckerman-Schpector A. J. (**2003**) Synthesis, characterization and crystallographic studies of three 2-aryl-3-methyl-4-aryl-1,3-thiazolium-5-thiolates. *Synthesis,* 5, 685-690.

33 Bourass M., Benjelloun A. T., Benzakour M., Mcharfi M., and Hamidi M. B. S., And Bouachrine M. (**2016**) Dft and td-dft calculation of new thienopyrazine-based small molecules for organic solar cells. *Chemistry Central Journal,* 10 (1), 1-11.

34 Boussaidi S., Zgou H., Eddiouane A., and Chaib H. (**2015**) New π -conjugated oligomers containing thiophene and phenylene rings with low band-gap for solar cell applications : A dft study. 5 (3), 1-9.

35 Zade S. S., Zamoshchik N., and Bendikov M. (**2011**) From short conjugated oligomers to conjugated polymers. Lessons from studies on long conjugated oligomers. *Accounts of Chemical Research,* 44 (1), 14-24.

36 Yang L., Feng J. K., and Ren A. M. (**2005**) Theoretical studies on the electronic and optical properties of two thiophene-fluorene based π-conjugated copolymers. *Polymer,* 46 (24), 10970-10981.

37 Shao S., Shi J., Murtaza I., Xu P., He Y., Ghosh S., Zhu X., Perepichka I. F., and Meng H. (**2017**) Exploring the electrochromic properties of poly(thieno[3,2-: B] thiophene)s decorated with electron-deficient side groups. *Polymer Chemistry,* 8 (4), 769-784.

38 Raftani M., Abram T., Bennani M. N., and Bouachrine M. (**2020**) Theoretical study of new conjugated compounds with a low bandgap for bulk heterojunction solar cells: Dft and td-dft study. *Results in Chemistry,* 1, 138277-138277.

39 Amine M., Hamidi M., Bouzzine S. M., Amine A., and Bouachrine M. (**2012**) A quantum chemical study on structural and electronic properties of new π-conjugated polymer named poly(4-methylthioazole-2,5-diyl). *Advanced Materials Letters,* 3 (1), 15-20.

40 Abram T., Zgou H., Bejjit L., Hamidi M., and Bouachrine M (**2014**) Design of new small molecules based on thiophene and oxathiazole for bulk heterojunction solar cells : A computational study. *IJARCSSE,* 4 (3), 742-750.

41 Liu S. (**2005**) Dynamic behavior of chemical reactivity indices in density functional theory: A bohn-oppenheimer quantum molecular dynamics study. *Journal of Chemical Sciences,* 117 (5), 477-483.

42 Parr R. G., Donnelly R. A., Levy M., and Palke W. E. (**2003**) Electronegativity: The density functional viewpoint. *The Journal of Chemical Physics,* 68 (8), 3801-3807.

43 Pearson R. G. (**1963**) Hard and soft acids and bases. *Journal of the American Chemical Society,* 85 (22), 3533-3539.

44 Parr R. G., and Pearson R. G. (**1983**) Absolute hardness: Companion parameter to absolute electronegativity. *Journal of the American Chemical Society,* 105 (26), 7512-7516.

45 Parr R. G., Szentpály L. V., and Liu S. (**1999**) Electrophilicity index. *Journal of the American Chemical Society,* 121 (9), 1922-1924.

46 Bedda T., Benharref A., and Elabdellaoui H. E. (**2014**) Theoretical study by d.F.T of region and stereo-selectivity of. *International Journal of Innovation and Applied Studies,* 8 (2), 720-727.

47 Chattaraj P. K., and Maiti B. (**2003**) Hsab principle applied to the time evolution of chemical reactions. *Journal of the American Chemical Society,* 125 (9), 2705-2710.

48 Street R. A. (**2011**) Localized state distribution and its effect on recombination in organic solar cells. *Physical Review B - Condensed Matter and Materials Physics,* 84 (7), 075208-075208.

49 Shakila G., Saleem H., and Sundaraganesan N. (**2017**) Ft-ir , ft-raman , nmr and u-v spectral investigation : Computation of vibrational frequency , chemical shifts and electronic structure calculations of 1-bromo-4-nitrobenzene. *World Scientific News,* 61 (2), 150-185.

50 Boukhssas S., Aouine Y., Alami A., El Hallaoui A., Tijani N., Yamni K., Zouihri H., Mrani D., and Lachkar. M. (**2018**) Hirshfeld surface analysis and dft calculations of 1-phenyl-n(benzomethyl)-n-({1-[(2-benzo-4-methyl-4,5-dihydro-1,3-oxazol-4yl)methyl]-1h-1,2,3-triazol-4-yl}methyl)methanamine.

51 Saranya M., Ayyappan S., Nithya R., Sangeetha R. K., and Gokila A. (**2018**) Molecular structure, nbo and homo-lumo analysis of quercetin on single layer graphene by density functional theory. *Digest Journal of Nanomaterials and Biostructures,* 13 (1), 97-105.

52 Scrocco E., and Tomasi J. (**1978**) Electronic molecular structure, reactivity and intermolecular forces: An euristic interpretation by means of electrostatic molecular potentials. *Advances in Quantum Chemistry,* 11, 115-193.

53 Barakat A., Al-Majid A. M., Soliman S. M., Mabkhot Y. N., Ali M., Ghabbour H. A., Fun H. K., and Wadood A. (**2015**) Structural and spectral investigations of the recently synthesized chalcone (e)-3-mesityl-1-(naphthalen-2-yl) prop-2-en-1-one, a potential chemotherapeutic agent. *Chemistry Central Journal,* 9 (1), 1-15.

54 Bourass M., Benjelloun A. T., Benzakour M., Mcharfi M., Jhilal F., Hamidi M., and Bouachrine M. (**2017**) The optoelectronic properties of organic materials based on triphenylamine that are relevant to organic solar photovoltaic cells. *New Journal of Chemistry,* 41, 13336-13346.

55 Bourass M., Touimi Benjelloun A., Benzakour M., Mcharfi M., Hamidi M., Bouzzine S. M., Serein-Spirau F., Jarrosson T., Lère-Porte J. P., Sotiropoulos J. M., and Bouachrine M. (**2015**) Theoretical

studies by using the dft and td-dft of the effect of the bridge formed of thienopyrazine in solar cells. *Journal of Materials and Environmental Science,* 6 (6), 1542-1553.

56 Scharber M. C., Mühlbacher D., Koppe M. D. P., Waldauf C., Heeger A. J., and Brabec C. J. (**2006**) Design rules for donors in bulk-heterojunction solar cells—towards 10 % energy-conversion efficiency. *Advanced Materials,* 18 (6), 789-794.

57 Lorente S. G. (**2015**) *Studies on organic solar cells based on small-molecules : Tetraphenyldibenzoperiflanthene and fullerene c 70.*

58 Nayak P. K., Garcia-Belmonte G., Kahn A., Bisquert J., and Cahen D. (**2012**) Photovoltaic efficiency limits and material disorder. *Energy and Environmental Science,* 5 (3), 6022-6039.

59 Manor A., and Katz E. A. (**2012**) Open-circuit voltage of organic photovoltaics: Implications of the generalized einstein relation for disordered semiconductors. *Solar Energy Materials and Solar Cells,* 97, 132-138.

60 Credgington D., and Durrant J. R. (**2012**) Insights from transient optoelectronic analyses on the open-circuit voltage of organic solar cells. *Journal of Physical Chemistry Letters,* 3 (11), 1465-1478.

61 Shuttle C. G., O'regan B., Ballantyne A. M., Nelson J., Bradley D. D. C., De Mello J., and Durrant J. R. (**2008**) Experimental determination of the rate law for charge carrier decay in a polythiophene: Fullerene solar cell. *Applied Physics Letters,* 92 (9), 90-93.

62 Scharber M. C., and Sariciftci N. S. (**2013**) Efficiency of bulk-heterojunction organic solar cells. *Progress in Polymer Science,* 38 (12), 1929-1940.

63 Sadiki Y. A., Bouzzine S. M., Bejjit L., Hamidi M., and Bouachrine M. (**2014**) Design and photovoltaic properties of new molecules based bithiophene for bulk heterojunction solar cells. *Mor. J. Chem,* 2 (1), 46-56.

64 Khan M. U., Khalid M., Ibrahim M., Braga A. A. C., Safdar M., Al-Saadi A. A., and Janjua M. R. S. A. (**2018**) First theoretical framework of triphenylamine-dicyanovinylene-based nonlinear optical dyes: Structural modification of π-linkers. *Journal of Physical Chemistry C,* 122 (7), 4009-4018.

65 Dessì A., Calamante M., Mordini A., Peruzzini M., Sinicropi A., Basosi R., Fabrizi De Biani F., Taddei M., Colonna D., Di Car A., Reginato G., and Zani L. (**2014**) Organic dyes with intense light absorption especially suitable for application in thin-layer dye-sensitized solar cells. *Chemical Communications,* 50 (90), 13952-13955.

66 Li M., Kou L., Diao L., Zhang Q., Li Z., Wu Q., Lu W., and Pan D. (**2015**) Theoretical study of acene-bridged dyes for dye-sensitized solar cells. *Journal of Physical Chemistry A,* 119 (13), 3299-3309.

67 Bourass M., Komiha N., Kabbaj O. K., Wazzan N., Chemek M., and Bouachrine M. (**2019**) The photophysical properties and electronic structures of bis [1] benzothieno[6,7-: D:6′,7′- d ′]benzo[1,2-b:4,5- b ′]dithiophene (bbtbdt) derivatives as hole-transporting materials for organic light-emitting diodes (oleds). *New Journal of Chemistry,* 43 (40), 15899-15909.

68 Rajamani T., and Muthu S. (**2013**) Electronic absorption, vibrational spectra, non-linear optical properties, nbo analysis and thermodynamic properties of 9-[(2-hydroxyethoxy) methyl] guanine molecule by density functional method. *Solid State Sciences,* 16, 90-101.

69 Zhang R., Du B., Sun G., and Sun Y. (**2010**) Experimental and theoretical studies on o-, m- and p-chlorobenzylideneaminoantipyrines. *Spectrochimica Acta - Part A: Molecular and Biomolecular Spectroscopy,* 75 (3), 1115-1124.